Mathematical Biosciences and Engineering

MBE, 17(6): 7302–7331.
DOI: 10.3934/mbe.2020374
Received: 19 August 2020
Accepted: 21 October 2020
Published: 27 October 2020

http://www.aimspress.com/journal/MBE

Research article

Research on the evaluation of the resilience of subway station projects to waterlogging disasters based on the projection pursuit model

Lanjun Liu[1], Han Wu[2,*], Junwu Wang[2] and Tingyou Yang[3]

[1] School of Civil Engineering and Architecture, Wuhan Institute of Technology, Wuhan 430070, China
[2] School of Civil Engineering and Architecture, Wuhan University of Technology, Wuhan 430070, China
[3] CCTEB Infrastructure Construction Investment Co., Ltd, Wuhan 430070, China

* **Correspondence:** Email: wu.han@whut.edu.cn; Tel: +8613407191168.

Abstract: To improve sustainable development, increasingly more attention has been paid to the evaluation of the resilience to waterlogging disasters. This paper proposed a projection pursuit model (PPM) improved by quantum particle swarm optimization (QPSO) for the evaluation of the resilience of subway station projects to waterlogging disasters. In view of the lack of research results related to the evaluation of the resilience of subway station projects to waterlogging disasters, 16 secondary indicators that affected the ability of subway station projects to recover from waterlogging disasters were identified from defense, recovery, and adaptability, for the first time. A PPM improved by QPSO was then proposed to effectively deal with the high-dimensional data about the resilience of subway station projects to waterlogging disasters. The QPSO was used to solve the best projection vector of the PPM, and interpolation algorithm was used to construct the mathematical model of evaluation. Finally, four station projects of Chengdu Metro Line 11 in China were selected for a case study analysis. The case study revealed that, among the secondary indicators, the emergency plan of construction order, the exercise frequency of emergency plans, and relief supplies had the greatest weights. The recovery was found to be the most important in the primary indicators. The values of the resilience of Lushan Avenue Station, Miaoeryan Station, Shenyang Road Station, and Tianfu CBD North Station to waterlogging disasters were found to be 2, 1.6571, 2.8318, and 3 respectively. This resilience ranking was consistent with the actual disaster situation in the flood season of 2019. In addition, the case study results showed that QPSO had the advantages of fewer parameter settings and a faster convergence speed as compared with PSO and the genetic algorithm.

Keywords: subway station project; waterlogging disasters; resilience capability; projection pursuit model; quantum particle swarm optimization

1. Introduction

With the increasingly severe global climate change and the acceleration of urbanization, many cities, especially those in developing countries, are suffering from waterlogging disasters [1]. Urban waterlogging disasters have become one of the practical problems that restrict the urbanization process and sustainable development of cities. Subway station projects are often located in low-lying areas of cities, and are typical disaster-bearing bodies of urban waterlogging disasters [2]. Because the construction site is an open environment, subway station construction is more vulnerable to rainstorms and waterlogging disasters. Improving the resilience of subway station projects has become a new way to handle waterlogging disasters and realize sustainable development.

Urban waterlogging refers to short-term intense rainfall in an urban area that exceeds the drainage capacity of the city, resulting in the formation of accumulated water [3]. There are noticeable differences in the toughness characteristics of research objects of different scales [4]. The city is a large-scale research object, whereas a subway station project is a small-scale research object. The management of waterlogging disasters in subway station projects is not only related to large-scale regional characteristics, such as the urban drainage system and catchment area [5], but also to the structural characteristics, construction technology, construction progress, and on-site management [6].

The concept of resilience originates from ecology and was referred to describe the ability of a specific system to restore its original or equilibrium state [7]. After 1970s, researches on resilience have spanned many disciplines and fields, including disaster science [8], social science [9], and engineering [10]. At present, scholars [11,12] generally believe that resilience has three basic elements, namely the system's defense ability against external interference, the ability to quickly restore balance after impact, and the ability to be adapted to similar risks.

Based on this, the resilience of subway station projects threatened by a waterlogging disaster can be considered as maintaining the main structure of the project and keeping the people, materials, and machines undamaged (defense), resuming the normal construction of the project in a timely manner after being damaged (recovery), and continuously improving the management ability and level of the construction site to better cope with future waterlogging disasters (adaptability). Resilience of subway station projects to waterlogging disasters is a comprehensive concept. Thus, one of the main contents of the present work is the accurate identification and construction of an evaluation index system for the ability of a subway station project to recover from a waterlogging disaster.

Owing to the complexity of the concept of resilience, there are many indicators that affect the resilience of subway station projects to waterlogging disasters, and the data are high-dimensional [6]. At present, fuzzy comprehensive evaluation and other functional mode evaluation methods are commonly used in disaster risk management and resilience evaluation [13]. However, they are characterized by the disadvantages of intense subjectivity during weight calculation and difficulty in processing high-dimensional data [6]. In the research of related topics, subjective weight calculation methods such as the analytic hierarchy process (AHP) [14] are typically used. Although expert experience is fully utilized in these methods, the calculation results are too subjective, and the weight calculation results are closely related to individual characteristics, such as the experience of experts who participate in the evaluation. Moreover, these methods have not effectively utilized a large amount of data in the evaluation of the ability of construction sites to recover after rainstorm waterlogging disasters.

The basic concept of PPM is to project high-dimensional data into a low-dimensional subspace via a precise mathematical combination, and to reflect the structural characteristics of the high-dimensional data by analyzing the data distribution structure in the low-dimensional space [15]. The PPM has been utilized increasingly more in the fields of risk assessment [16] and decision [17] to effectively take care of high-dimensional data. It can be used to directly calculate the objective weight of indicators from the characteristics of sample data [16]. Complex evaluation samples can also be directly synthesized into one-dimensional projection vectors for evaluation via the inner product of the optimal projection vectors and evaluation index vectors [17]. Another main effort of the present study is the proposal of an improved PPM based on QPSO to evaluate the resilience of subway station projects to rainstorm waterlogging disasters. The key to the correct use of the PPM is to solve the optimal projection vector, which is a complex nonlinear optimization problem [16–18].

PSO was originally proposed by Eberhart and Kennedy in 1995 [19], and its basic concept originates from the study of birds' foraging behavior. PSO is commonly used in the solution of complex nonlinear optimization problems [20]. However, the search space of PSO is limited, and it easily falls into the local extremum [21]. These shortcomings limit its further and wider use. Based on the standard PSO, Sun et al. [22] proposed the QPSO. During the process of particle convergence, particle i continues approaching P_i until it falls within P_i. From the perspective of quantum mechanics [23], there is an attractive potential at point P_i in the process of convergence, which attracts particles to converge to P_i and aggregates the entire population. Particles in a quantum bound state can appear at any space point with a certain probability [24]. Therefore, particles can search in the entire solution space and better convergence can be achieved.

The main author of this article have used the PPM to analyze the waterlogging risk of deep foundation pit engineering [6]. The research of this new paper is a great improvement on the basis of that paper. First of all, the previous research objects were rough and not detailed enough. In this paper, resilience was chosen as the research object rather than risk. Then, the previous research only used the PSO to optimize the PPM. In this manuscript, QPSO was used to optimize the PPM, for the first time. Compared with PSO and GA, it showed that QPSO was advanced. Finally, this manuscript analyzed the calculation error, calculation stability and parameter analysis of each PPM optimized by QPSO in detail, which was not in previous papers.

The contributions of this paper are as follows: (1) In this paper, from the three aspects of defense, recovery, and adaptability, the evaluation index of resilience of waterlogging disaster in subway stations was constructed, for the first time. In the process of establishing the index system, not only the multi-disciplinary professional knowledge was comprehensively applied, but also the characteristics of waterlogging disasters and the project management of subway stations were fully considered. (2) The PPM, QPSO, and an interpolation algorithm were used to construct the evaluation model, for the first time. In this model, the PPM was utilized to effectively deal with the high-dimensional data, QPSO was used to solve the best projection vector of the PPM, and interpolation algorithm was used to construct the mathematical model of evaluation. (3) According to a case study, the key factors of the resilience were revealed to be the emergency plan of construction order, the exercise frequency of emergency plans, and relief supplies. The resilience levels of Lushan Avenue Station, Miaoeryan Station, Shenyang Road Station, and Tianfu CBD North Station were found to be 2, 1.6571, 2.8318, and 3, respectively. In addition, the case study results showed that QPSO had the advantages of fewer parameter settings and a faster convergence speed as compared with PSO and the genetic algorithm (GA). (4) The parameters of the random sampling number of the interpolation algorithm were analyzed. It was preliminarily considered that good calculation stability and progress could be achieved by taking 100 samples from each interval. The parametric analysis of the random sampling number of the interpolation algorithm was another difference between the research presented in this paper and other published research results based on the PPM.

The organizational structure of the remainder of this paper is as follows. Section 2 summarizes the related work. Section 3 introduces the research methods in detail, including the construction of the index system and the evaluation model based on the PPM improved by QPSO. Section 4 presents a case study. In section 5, the computing performances of different algorithms are compared, and the random sampling numbers of interpolation algorithms are analyzed. Finally, section 6 provides relevant conclusions of this research.

2. Related work

While a substantial amount of research has been conducted on the risk assessment or vulnerability assessment of rainstorm waterlogging disasters, there has been little research on disaster resilience. Previous studies have often regarded disaster resilience as a component of disaster risk or vulnerability. The relationship between the disaster recovery ability and disaster risk was implicitly expressed through disaster loss [3]. Zeng and Huang [25] cursorily combined disaster resilience and disaster risk into the concept of disaster severity in their study, so this work did not accurately and scientifically reveal the impacts of disaster resilience on catastrophe severity and disaster risk. Some scholars have acknowledged the importance of disaster recovery ability evaluation in disaster management research. Lo et al. [26] studied the resilience in Tianjin China for waterlogging disasters in detail, and the research results revealed that the financial situation and educational level of the residents were the most critical factors. It was therefore suggested that the local government in Tianjin put forward targeted disaster prevention strategies from these two aspects. Lyu et al. [27] emphasized the adaptability of cities to climate change, which was an important part of sustainable urban development. Cui and Li [28] believed the research on resilience to be the frontier of disaster management research. The disaster resilience of urban communities was considered from the society, economy, and natural capital. In addition, the paper established a fuzzy comprehensive evaluation model.

At present, functional model assessment methods, such as fuzzy comprehensive assessment, are often adopted for the risk assessment of rainstorm waterlogging disasters. Yu et al. [2] established a waterlogging risk evaluation model of urban subway stations via a fuzzy comprehensive evaluation method. In this paper, the relationship between the index risk level and disaster risk level must be artificially preset, thereby reducing the research and popularization value. Liu et al. [13] used the AHP and fuzzy variable set theory to study flood catastrophes in Henan Province, China. However, the AHP is too subjective, and the choice of different experts has a pronounced influence on the weight calculation and final risk analysis. Moreover, the relationship between the index risk level and disaster risk level needs to be preset. Based on the formation mechanism of flood disasters, Li et al. [14] established an index system of flood risk assessment in the middle and lower reaches of the Yangtze River in China, and determined the weights of the index by the AHP. To the best of the authors' knowledge, research on the evaluation of the resilience of subway station projects to waterlogging disasters has not yet been reported.

In recent years, the PPM has been applied increasingly more in the risk assessment and decision-making fields that involve multi-factor influence and high-dimensional data. To effectively deal with complex multi-factor problems in the assessment of karst water pollution, Wang et al. [29] constructed a PPM improved by the GA, in which the GA was used to find the best projection direction of the PPM. Gong et al. [30] used the PPM to effectively determine the best mixture ratio of cement materials. By projecting high-dimensional data into low-dimensional space, they successfully transformed the typical multi-objective optimization problem into two single-objective optimization problems. Delta. Zhi et al. [16] established a PSO combined with PPM to analyze the flood risk in urban areas. The case study results demonstrated that the new algorithm could deal with multi-source heterogeneous data, and the objective weight of each index was successfully determined from this high-dimensional information. Lan and Huang [31] adopted the water cycle algorithm to optimize the PPM, and the square of each element in the best projection vector was considered to be the objective weight of the element in a seawall safety evaluation index.

The key to the effective use of the PPM is the selection of an appropriate method to solve the optimal projection vector, and meta-heuristic algorithms such as the GA or PSO are often used for this task. However, QPSO is a new intelligent optimization algorithm that has the advantages of fewer parameters, easy implementation, and better convergence [32]. Meng et al. [23] used QPSO to predict the economic load of power plants, and QPSO was found to be superior to the GA, immune algorithm (IA), and other versions of PSO in a case study. Zhang et al. [24] adopted a multi-objective QPSO to study the route design of railway freights, and case study results revealed that, as compared with other classical optimization algorithms, the best Pareto front calculated by the QPSO was closer to the real Pareto front of railway freight route design. Fang et al. [33] summarized the latest research progress of QPSO and noted that the excellent search ability of QPSO has been verified in various application tests. Fu et al. [34] designed a new unmanned aerial vehicle route planner based on the improved QPSO, and their experimental results demonstrated that QPSO performed better than the GA, differential evolution (DE), and classical PSO. According to the author's literature search, no scholars have used QPSO to optimize the PPM. Yang et al. [35] used the QPSO algorithm to effectively solve the fuel and time optimization problems in the long-distance fast cooperative rendezvous between two spacecraft. The research results showed that compared with other common algorithms, the QPSO algorithm was able to effectively reduce time consumption and ensure the stability of calculation. Talbi and Draa [36] found that quantum-inspired evolutionary algorithm was more effective than other algorithms.

3. Methodology

3.1. Index system of waterlogging disaster resilience capability of subway station projects

3.1.1. Determination of the factors of the waterlogging disaster resilience capability

According to the definition of resilience put forward in the introduction, three attributes of resistance, resilience, and adaptability are discussed in this section, and an evaluation index system of the resilience of subway station projects to waterlogging disasters is established.

(1) Resistance refers to the ability of the subway station project to reduce waterlogging disaster losses.

In general, the public emergency response ability of people over 50 years old has notably declined [37], and these citizens are more vulnerable in emergencies such as natural disasters. Therefore, in subway station projects, the greater the proportion of construction workers over the age of 50, the weaker their resistance to waterlogging disasters. The water retention ability of subway station projects primarily depends on the retaining wall around the deep foundation pit, and the height of the retaining wall directly determines whether the water accumulated during a rainstorm can easily get into the construction site. The higher the height of the retaining wall, the stronger the resistance to waterlogging disasters. The height of the retaining wall therefore reflects the engineering structural characteristics of the resistance of a subway station project to waterlogging disasters.

From the perspective of the water cycle [14], the formation of a waterlogging disaster is related not only to the water retention capacity of the disaster-bearing body, but also to the drainage speed [13]. The higher the density of drainage pipes around the subway station project, the faster the regional drainage speed, and the stronger the resistance to waterlogging disasters [2]. In addition, the higher the pump density in the construction site, the easier it is tantamount to discharge accumulated water, and the stronger the resistance to rainstorm waterlogging disasters. When a subway station project is in different construction stages, there are great differences in the statuses of the talents, machinery, and flood control measures at the construction site. Therefore, it is necessary to fully consider the influences of diverse construction stages on the resistance of subway station projects to waterlogging disasters. In addition, flood control emergency plans are at the heart component of emergency management in this situation.

(2) Resilience refers to the ability of a subway station project to change from an unbalanced state to a balanced state in a timely manner. It is intuitively expressed as the ability of a subway station project to eliminate the adverse effects caused by waterlogging disasters and restore the normal construction order.

Exercises of the emergency waterlogging disaster plan before a disaster occurs can reveal the rationality of the plan and significantly improve the command and communication efficiency of flood control and disaster relief [28], which has a key impact on ensuring the efficient implementation of the plan and successful relief work [38]. A large number of professional rescue workers and sufficient relief materials are the foundations and keys to successfully carrying out emergency relief work [39]. At present, the expenses related to disaster management in the subway station project management are mainly related to safe and civilized construction costs. The rate of safe and civilized construction therefore reflects the project management characteristics of the resilience of subway station projects to waterlogging disasters.

After a waterlogging disaster occurs, the project managers of subway stations often implement the disaster emergency management plan on the construction site. This plan mainly includes plans for the restoration of construction order, the construction working conditions, and the construction work, as well a crisis intervention system and its implementation. Among them, the construction order restoration plan is the center of the disaster emergency management plan. In addition, when a subway station project recovers from a rainstorm waterlogging disaster, it is necessary to discharge the flood water from the inside the project to the periphery. Therefore, the water pump density in the surrounding urban areas of the subway station project is another important factor that affects the resilience of the subway station project to waterlogging disasters. The higher the density of water pumps in the surrounding urban areas, the easier it is meant for the accumulated water to be discharged, and the faster the subway station project can be restored. In other words, the resilience of urban areas restricts the resilience of the subway station project.

(3) Adaptability refers to the ability of a subway station project to adjust itself in response to future rainstorm waterlogging events of different grades.

Considering the one-off characteristics of subway station project management, the adaptability of a subway station project to rainstorm waterlogging primarily refers to the self-adjustment ability of the project after experiencing a waterlogging disaster, the constant adjustment of the project management strategy, and updating the site construction technology to cope with the next rainstorm. In addition, project managers' understanding of rain and flooding is also an important factor by which to measure urban adaptability [26]. A good education level of project managers often indicates good disaster awareness, and project managers with good disaster awareness can take effective measures in time to avoid adverse effects in the face of rain and flood disasters, thereby ensuring the normal construction of subway station projects when disasters occur.

3.1.2. Construction of an evaluation index system

Based on the analysis presented in section 3.1.1, an index system was constructed for the evaluation of the resilience of subway station projects to waterlogging disasters, as showed in Table 1.

Among them, the secondary indicators R15, R16, R23, R25, R32, R33, and R34 are qualitative, while the others are quantitative. The data on the qualitative indicators are obtained by questionnaire surveys, while the data on quantifiable indicators are obtained by field investigations, the consultation of project management data, referring to standard calculations, and other methods. It is useful to noting that qualitative indicators have no units of measure. The smaller the cost index, the better. The effect index is only the opposite.

Table 1. Evaluation index system of waterlogging disaster resilience capability.

Primary Indicators	Secondary Indicators	Type	Unit
R1: Defense	R11: Proportion of workers over 50 years old	Cost	%
	R12: Height of retaining wall	Value	m
	R13: Density of surrounding drainage pipes	Value	km/km^2
	R14: Water pump density on the construction site	Value	$/km^2$
	R15: Construction stage	Cost	–
	R16: Preparation of flood control emergency plan	Cost	–
R2: Recovery	R21: Exercise frequency of emergency plan	Value	times/year
	R22: Proportion of professional rescue workers	Value	%
	R23: Relief supplies	Value	–
	R24: Rate of safety and civilized construction measures	Value	%
	R25: Emergency plan of construction order	Cost	–
	R26: Water pump density in the surrounding urban area	Value	$/km^2$
R3: Adaptive	R31: Proportion of college students in project management personnel	Value	%
	R32: Summary of post-disaster management	Cost	–
	R33: Post-disaster technology update	Cost	–
	R34: Post-disaster site rearrangement	Cost	–

3.1.3. Assessment standard of waterlogging disaster resilience capability

There currently exists no unified grading standard of waterlogging disaster resilience capability in subway station projects [40]. According to the needs of project management practice, the resilience capability was divided into five grades, namely extremely low risk (I), low risk (II), moderate risk (III), high risk (IV), and extreme risk (V). Extremely low risk indicates that the project has a good ability to recover from waterlogging, and no further measures are necessary. Low risk indicates that the project has a nice ability to recover from waterlogging, but full attention should be paid to the possible losses. Moderate risk indicates that the recovery ability of this project is average, so it is necessary to formulate relevant measures to improve the recovery ability. High risk indicates that the recovery ability of this project is poor, and the construction work can be continued after expert argumentation. Finally, extreme risk indicates that the ability of this project to recover from rainstorm waterlogging is very pitiable, and the construction task should be suspended immediately.

In addition, five grades were used to divide the recovery ability in this paper, but obviously it had feasible alternatives. It is possible to divide the resilience into three levels, four levels and six levels.

The basis for the evaluation grade division of specific indicators must be established according to the engineering characteristics and project management needs of the case study objects. Table 2 presents the grading basis of the index system of the resilience of subway station projects of Chengdu Metro Line 11 in China. The classification basis of qualitative indicators was primarily the opinions of experts, and the scoring interval [0, 100] was divided into five sub-intervals. The classification basis of quantitative indicators was primarily the relevant Chinese national codes (Technical Code for Urban Waterlogging Prevention (GB 51222-2017), Code for Design of Urban Flood Control Projects (GB/T 50805-2012), and Code for Risk Management of Underground Engineering Construction of Urban Rail Transit (GB 50652-2011)) and the stations on Chengdu Metro Line 11.

Table 2. Assessment standards of the evaluation index system.

Secondary Indicators	I	II	III	IV	V
R11	[0,5)	[5,10)	[10,20)	[20,50)	[50,100]
R12	[1.8,+∞)	[1.2,1.8)	[0.6,1.2)	[0.4,0.6)	[0,0.4)
R13	[8,+∞)	[4,8)	[2,4)	[1,2)	[0,1)
R14	[100,+∞)	[80,100)	[40,80)	[20,40)	[0,20)
R15	[0,20)	[20,40)	[40,60)	[60,80)	[80,100]
R16	[0,20)	[20,40)	[40,60)	[60,80)	[80,100]
R21	[8,+∞)	[4,8)	[2,4)	[1,2)	[0,1)
R22	[40,100]	[30,40)	[10,30)	[5,10)	[0,5)
R23	[0,20)	[20,40)	[40,60)	[60,80)	[80,100]
R24	[5,20]	[4,5)	[2,4)	[1,2)	[0,1)
R25	[0,20)	[20,40)	[40,60)	[60,80)	[80,100]
R26	[50,+∞)	[40,50)	[20,40)	[10,20)	[0,10)
R31	[60,100]	[40,60)	[20,40)	[10,20)	[0,10)
R32	[0,20)	[20,40)	[40,60)	[60,80)	[80,100]
R33	[0,20)	[20,40)	[40,60)	[60,80)	[80,100]
R34	[0,20)	[20,40)	[40,60)	[60,80)	[80,100]

3.2. The evaluation method based on the PPM improved by QPSO

3.2.1. Projection pursuit model

Artificial intelligence algorithms such as data mining are widely used in engineering field [41]. The PPM, a typical data mining algorithm, contains the following unique advantages in overcoming the problems of small sample numbers and high-dimensional data. (1) It can overcome the "curse of dimension". It refers to the sparse distribution of data in high-dimensional space when the dimension of the data is too high and there are many sample points. PPM increases the density of sparse data points by projecting high-dimensional data onto a low-dimensional subspace so that the structure or characteristics of the data in the projection space can be discovered. This is suitable for data with a non-normal distribution or little prior information [16]. (2) After the PPM is implemented, it can eliminate the interference of variables that are unrelated to, or have little relationship with, the structural features of the original data. By finding the best projection that meets the projection target, the influences of some unimportant variables can be eliminated [17].

The basic workflow of the PPM is as follows.

(1) Construction of a projection index function

The PPM synthesizes m-dimensional data $\{x(i,j)|j = 1,2,\cdots,m\}$ into a one-dimensional projection value $z(i)$ with $\vec{\mathbf{a}} = \{a(1), a(2), \cdots, a(m)\}$ as the projection direction [29]:

$$\mathrm{z}(i) = \sum_{j=1}^{m} a(j)x(i,j) \tag{1}$$

It is worth noting that $\{a(1), a(2), \cdots, a(m)\}$ is the unit length vector, which is the most important constraint in PPM.

$$\sum_{j=1}^{m} a^2(j)=1 \tag{2}$$

where $0 \leq a(j) \leq 1$, $j = 1,2,\cdots,m$.

When determining the projection index, it is required that the local projection points of the projection value $\mathrm{z}(i)$ be as dense as possible. Therefore, the constructed projection function [29] is:

$$\mathbf{Q}(a) = S_z D_z \tag{3}$$

where S_z is the standard deviation of the projected value $\mathrm{z}(i)$ [16], and D_z is the local density of the projected value $\mathrm{z}(i)$ [16]. These parameters are respectively calculated as:

$$S_z = \sqrt{\sum_{i=1}^{n} (z(i) - \bar{z})^2/(n-1)} \tag{4}$$

$$D_z = \sum_{i=1}^{n} \sum_{j=1}^{m} \big(R - r(i,j)\big) \cdot o\big(R - r(i,j)\big) \tag{5}$$

where, $\bar{z}$ is the average value of sequence $z(i)$, R is the window radius of local density, $r(i,j)$ is the distance between samples, and $o\big(R - r(i,j)\big)$ is a unit step function. Its value is 1 if $R - r(i,j) \geq$

0, and its value is 0 if $R - r(i,j) < 0$.

(2) Optimization of the projection exponential function

When the projection index function determines gets the maximum value, the corresponding $\vec{\mathbf{a}}$ direction can best reflect the optimal projection direction of data features. Therefore, the problem of finding the optimal projection direction is transformed into a problem of nonlinear optimal solution [30]:

$$\begin{cases} \max: \mathbf{Q}(a) = S_z D_z \\ \mathrm{s.t}: \sum_{j=1}^{m} a^2(j) = 1 \end{cases} \tag{6}$$

where $0 \le a(j) \le 1,\ j = 1,2,\cdots,m$.

Similarly, when the projection index function determines the minimum value, the corresponding $\vec{\mathbf{a}}$ direction can best reflect the optimal projection direction of data characteristics. Therefore, the problem of finding the optimal projection direction is transformed into a problem of nonlinear optimal solution [30]:

$$\begin{cases} \min: \mathbf{Q}(a) = 1/S_z D_z \\ \mathrm{s.t}: \sum_{j=1}^{m} a^2(j) = 1 \end{cases} \tag{7}$$

3.2.2. Quantum particle swarm optimization

In the classical PSO, the convergence of particles is achieved in the form of an orbit. During the process of searching, particles have the limit of a maximum speed [42]. Therefore, the search area is bounded every time, so the classical PSO cannot globally converge with probability. The QPSO holds that particles exhibit quantum behavior, and when each particle moves in the search space, there exists a delta-potential well-centered on *Pbest* [22]. Particles in quantum space satisfy completely different properties of the aggregation state, and there is no definite trajectory when particles move, and this enables particles to explore and find the global optimal solution in the entire feasible solution space. Therefore, the global search ability of the QPSO is far superior to that of the classical PSO [32–34].

In the QPSO, δ potential drop is introduced, and it is assumed that particles are in δ potential drop with point p as the center. Because the velocity and position of particles cannot be simultaneously determined in quantum space, the state of particles is expressed by the wave function $\phi(Y) = \frac{1}{\sqrt{L}} e^{\frac{-|Y|}{L}}$, where $L = \frac{1}{\beta} = \frac{h^2}{mr}$.

Let the attractor $P_i = (P_{i1}, P_{i2}, \cdots, P_{iN})$, and establish a one-dimensional δ potential drop with P_n as the coordinate and $P_{i,j}$ as the center. For $P_{i,j}$, there are particles i in each dimension [22]:

$$\phi\left[x_{i,j}(t+1)\right] = \frac{1}{\sqrt{L_{i,j}(t)}} \exp\left[-\frac{\left|x_{i,j}(t+1) - P_{i,j}(t)\right|}{L_{i,j}(t)}\right] \tag{8}$$

The position equation [23] is:

$$x_{i,j}(t+1) = P_{i,j}(t) \pm \frac{L_{i,j}(t)}{2} \operatorname{In}\left(\frac{1}{u_{i,j}(t)}\right) \tag{9}$$

where $u_{i,j}(t) \sim u(0,1)$.

According to the characteristic length $L_{i,j}(t)$ of particle δ potential well, Sun et al. [22] designed a new parameter control method based on global level, which was the mean best position (mbest). The new method can effectively optimize the parameters of $L_{i,j}(t)$. The mbest is introduced and defined as follows [22]:

$$mbest = \frac{1}{M}\sum_{i=1}^{M} P_i(t) = \left(\frac{1}{M}\sum_{i=1}^{M} P_{i,1}(t), \frac{1}{M}\sum_{i=1}^{M} P_{i,2}(t), \cdots, \frac{1}{M}\sum_{i=1}^{M} P_{i,n}(t)\right) \tag{10}$$

According to the above definition, the $L = \frac{1}{\beta} = \frac{h^2}{mr}$ in quantum mechanics is further expressed in QPSO as $L_{i,j}(t)$. $L_{i,j}(t)$ is the characteristic length of δ potential well of particle i in the t iteration of the j-th dimension search space, which can be expressed as:

$$L_{i,j}(t) = 2\alpha\left|mbest_j(t) - x_{i,j}(t)\right| \tag{11}$$

Introducing Eq (11) into Eq (9), the position updating equation of QPSO algorithm defined based on the mean best position is obtained [22]:

$$x_{i,j}(t+1) = P_{i,j}(t) \pm \alpha\left|mbest_j(t) - x_{i,j}(t)\right| * \operatorname{In}\left(\frac{1}{u_{i,j}(t)}\right) \tag{12}$$

where α is the contraction and expansion factor. The PSO applied to Eq (12) is called QPSO.

It is worth mentioning that many scholars have put forward some new location update methods of the QPSO algorithm [43–45]. In this paper, the location update method of the QPSO algorithm we chose is the classic location update method. The research purpose of this paper focused on introducing meta-heuristic algorithm to evaluate the resilience of waterlogging disaster in subway stations, which is the typical engineering problem. In the following research, the authors will compare the computational performance of different meta-heuristic algorithms, especially the latest meta-heuristic algorithm.

3.2.3. The construction of evaluation method

Step 1. Data collection and preprocessing.

According to the grading standards of each index evaluation grade in Table 2, n standard samples are generated in each grade interval by using the random sampling method [46], and $p * n$ standard sample sets $\mathbf{X_1} = \left[x_{ij}\right]_{(p*n)\times m}$ are obtained, where x_{ij} is the j index value of the i-th evaluation object, m is the number of evaluation indexes, and p is the resilience. In this study, resilience is divided into five grades, so $p = 5$. $\mathbf{Y} = \left(y_1, y_2, \cdots, y_{p*n}\right)^{\mathrm{T}}$ is the resilience grade of each standard sample in $\mathbf{X_1}$.

The evaluation sample set $\mathbf{X_2} = \left[x_{ij}\right]_{k\times m}$ of k evaluation objects is obtained by field investigations and questionnaire surveys.

A calculation sample set $\mathbf{X} = \begin{Bmatrix} \mathbf{X_1} \\ \mathbf{X_2} \end{Bmatrix} = \left[x_{ij}\right]_{(p*n+k)\times m}$ is established for the calculation of the optimal projection vector and projection value.

All indicators must first be normalized [47]. And the benefit-based indicators [40] are normalized as follows:

$$x_{ij}^* = \frac{x_{ij} - \min(x_j)}{\max(x_j) - \min(x_j)} \tag{13}$$

The cost-based indicators [40] are normalized as follows:

$$x_{ij}^* = \frac{\max(x_j) - x_{ij}}{\max(x_j) - \min(x_j)} \tag{14}$$

where x_{ij}^* represents the standardized evaluation index value, and $\max(x_j)$ and $\min(x_j)$ respectively represent the maximum and minimum values of the j-th index. The data collection and preprocessing in this step is a part of data set in Figure 1.

Step 2. Calculate the weights and projection values by the PPM and QPSO.

The specific implementation steps of solving the optimal projection function in PPM by using QPSO are shown in Figure 1. This paper gives the detailed steps of the PPM optimized by QPSO in combination with Figure 1.

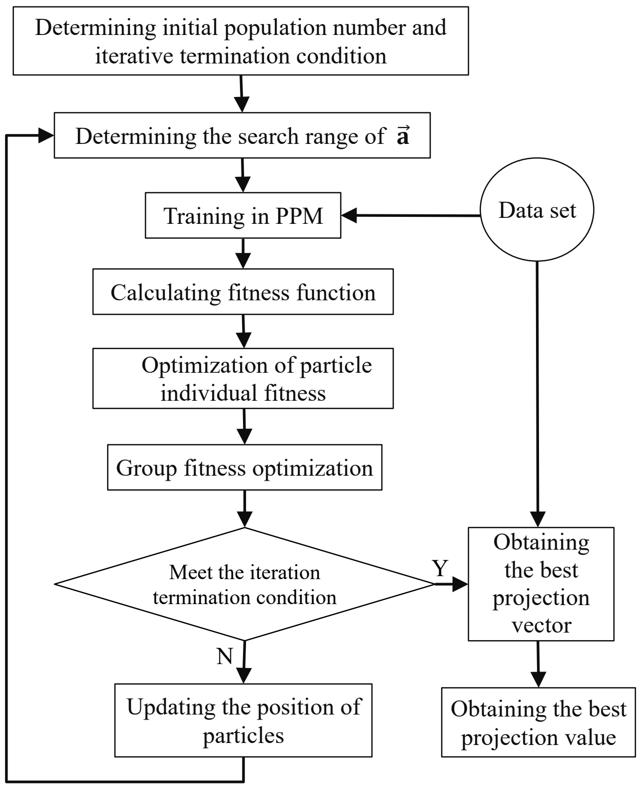

Figure 1. Optimized flow chart.

(1) The normalized calculation sample set $\left[x_{ij}^{*}\right]_{(p*n+k)\times m}$ is used to construct the projection index function $z(i)$ according to Eq (1). According to Eq (6) or (7), the search range of $\vec{\boldsymbol{a}}$ can be determined, and the initial population number and iteration termination conditions can be determined according to the characteristics of the research object.

(2) In this paper, an index is used to correspond to one dimension of particle vector. Eqs (3)–(5) are used to find the maximization objective function $\boldsymbol{Q}(a)$ in Eq (6) or the minimization objective function $\boldsymbol{Q}(a)$ in Eq (7). The QPSO is used to solve the function $\boldsymbol{Q}(a)$ in Eq (6) or (7). The calculation process of QPSO must be analyzed in detail to ensure that the objective function is optimized.

(3) If the QPSO does not meet the convergence condition, the position of particles will be updated. When the QPSO reaches the convergence condition, the best projection direction $\boldsymbol{a}^{*}$ and the projection value $\boldsymbol{Z}(i)$of the computation set can be obtained. In the calculated set of projection values $\boldsymbol{Z}(i),\ i=1,2,3,\cdots,p*n+k$. The projection value $\boldsymbol{Z}(i)$ of the calculation set includes the projection value $\boldsymbol{Z}_1(i)$ of the standard sample set and the projection value $\boldsymbol{Z}_2(i)$ of the evaluation index set.

(4) Squaring each element in the best projection vector $\boldsymbol{a}^{*}$ yields the objective weight of each index [31], which is the best projection value in the Figure 1.

Step 3. Determine the evaluation level by the interpolation algorithm

(1) According to the principle of PPM, the projection value is calculated as discrete data. Interpolation adds continuous function on the basis of discrete data, so that this continuous curve passes through all given discrete data points. Interpolation method has strong applicability in projection pursuit algorithm. According to the projection value $\boldsymbol{Z}_1(i)$ of the standard sample set and its preset risk grade $\boldsymbol{Y}_1(i)$, the mathematical model of risk evaluation is constructed by the interpolation method [46]:

$$\boldsymbol{Y}=f(\boldsymbol{Z}_1) \tag{15}$$

(2) By introducing the projection value $\boldsymbol{Z}_2(i)$ of the evaluation sample set into the mathematical model $\boldsymbol{Y}=f(\boldsymbol{Z}_1)$, the waterlogging risk level of each evaluation sample can be calculated.

4. Case study

4.1. Background and data source

Chengdu Rail Transit Line 11 is placed in Chengdu, China. It has a total length of 22.0 km and includes 19 underground subway stations. Construction of this project officially started in June 2017 and was expected to be completed in June 2020. Chengdu is in a humid subtropical climate zone with abundant rainfall, the average annual rainfall is 879.3 mm, the maximum annual rainfall is 1343.3 mm, the annual rainfall days are 141, and the maximum daily rainfall is 167.6 mm. Rainfall is mainly concentrated from May to September, which accounts for 84.1% of the annual rainfall. According to the Chengdu water resources bulletin and local yearbook, there were 28 serious regional waterlogging disasters in Chengdu from 2000 to 2018.

Obtaining engineering data is always one of the main difficulties in engineering papers. Before 2000, China did not establish relevant data release mechanism. During our writing, the data of 2019 could not be obtained. Probably due to the COVID-19, the Chengdu Government of China postponed the release of the data of rainstorm waterlogging disasters in 2019. During the authors' writing, only the engineering data related to the subway station project in 2018 was able to be obtained.

Lushan Avenue Station, Miaoeryan Station, Shenyang Road Station, and Tianfu CBD North Station are four typical station projects of the Chengdu Rail Transit Line 11 Project. The four stations selected in this case study include the core urban area, CBD area under construction, suburban development zone and suburban rural area of Chengdu, and cover almost all the common surrounding environments of subway station construction. Among these four stations, there are China Construction Third Bureau Infrastructure Construction Investment Co., Ltd. and China Construction Railway Investment and Construction Group Co., Ltd., and Southwest Branch of China Construction Third Bureau Group Co., Ltd. The management level and technical level of these construction enterprises are quite different. The geological conditions of these four stations are different, almost including the types of geological conditions of subway stations in Chengdu. In addition, this study had tried to collect the data of subway stations under construction in Wuhan, Chongqing, Shenzhen, Tianjin and other places. Due to the lack of cooperation with relevant construction enterprises, it was difficult to obtain the detailed information of the site.

Twenty experts were invited to score the qualitative indexes in the evaluation index system of the waterlogging disaster resilience capabilities of these four station projects. The selection criteria of the twenty invited experts were mainly considered from five aspects, namely their work unit, title, experience, time working in this project, and age [48]. The 20 experts in this paper are all in the field of civil engineering.

Table 3. Results of 20 experts on various qualitative indexes of Lushan Avenue Station.

No.	R15	R16	R23	R25	R32	R33	R34
Expert 1	20	85	60	70	90	30	10
Expert 2	15	80	65	75	95	40	5
Expert 3	20	85	65	70	85	35	10
Expert 4	20	90	60	75	85	40	15
Expert 5	15	85	65	75	85	35	15
…	…	…	…	…	…	…	…
Expert 16	15	90	65	70	90	30	20
Expert 17	10	75	60	75	80	25	10
Expert 18	20	85	65	70	90	30	15
Expert 19	15	80	60	75	90	30	10
Expert 20	20	90	65	75	90	40	20
Average score	17.5	83.5	63.5	73.5	89	34.5	13.5

The reliability of the questionnaire survey results of Lushan Avenue Station was tested by SPSS 22 software and the value of Cronbach’s α was found to be 0.703. This exceeded the required minimum value of 0.6 [49], thereby indicating that the questionnaire survey results were reliable. Due to spatial constraints, the scoring results of the 20 experts on the qualitative indexes of Miaoeryan Station, Shenyang Road Station, and Tianfu CBD North Station are not reported here. However, the reliabilities of the questionnaire surveys were also tested by SPSS 22 software, and their respective Cronbach’s α values were 0.728, 0.706, and 0.968. This analysis verifies that the reliability of the qualitative index scores for the case study conducted in this work was good and reasonable.

The quantitative indicators were selected by consulting project management data, on-site investigation, and calculation. According to the project management requirements of Chengdu Rail Transit Line 11, the upper limits of the quantifiable indexes R12, R13, R14, R21, and R26 were respectively set to 18, 80, 500, 80, and 500.

Table 4. Indicator' scores of the four evaluation objects.

Secondary Indicators	Lushan Avenue Station	Miaoeryan Station	Shenyang Road Station	Tianfu CBD North Station
R11	6.82	3.91	5.54	9.09
R12	1	1.2	1	1.6
R13	21	2	27	11.2
R14	46.4	53.7	21.875	63.6
R15	17	54.83	58.67	64.38
R16	84.5	33	39.5	57
R21	4	4	4	4
R22	21.35	16.53	16.53	10.87
R23	63	40.5	24.5	13
R24	2.5	2.5	2.5	2.5
R25	73	22	44.5	60.7
R26	71.31	37.42	15.73	53.26
R31	36.59	27.03	19.61	20.83
R32	88	46.5	22	17
R33	33.5	52.5	55	84.5
R34	13	40.5	56.5	24.5

4.2. *Mathematical evaluation model of waterlogging disaster resilience capability with the interpolation algorithm*

The calculation steps outlined in section 3.2.3 were used to construct the model.

Step 1. Data collection and preprocessing.

According to the evaluation grading standards of each secondary index in Table 2, 100 standard evaluation objects [6,42] were generated in five evaluation grade intervals by the random sampling method, and the standard sample set $\mathbf{X_1} = \left[x_{ij}\right]_{500\times16}$ was obtained. The resilience grade $\mathbf{Y_1} = (y_1, y_2, \cdots, y_{500})^{\mathrm{T}}$ of each standard evaluation object in the standard sample set was known. According to the data of $\mathbf{X_2} = \left[x_{ij}\right]_{4\times16}$ of each unit to be evaluated presented in Table 4, the sample set $\mathbf{X} = \begin{Bmatrix}\mathbf{X_1}\\ \mathbf{X_2}\end{Bmatrix} = \left[x_{ij}\right]_{504\times16}$ was substituted into a self-made program based on MATLAB R2016a software for calculation.

The parameter setting of QPSO is relatively simple, and only two calculation parameters, namely the population number and convergence condition, need to be set [32]. Referring to the parameter setting in previous researches [34,50], QPSO parameters in this case study were set as follows: the contraction and expansion factor $\alpha = 0.4$, initial population number $N = 100$, and the iterative termination condition was when the number of iterative calculations reached 1000 or the minimum accuracy reached 0.00001. Like previous studies [32–36], the parameter setting of this paper was conservative to ensure that the QPSO could converge effectively under the current parameter setting. In the research of algorithm, the parameters of QPSO should be analyzed to find the best parameter setting. However, when solving engineering problems, the parameter setting method in this paper is feasible. In different cases, different input data sets, or different index systems, the best parameter settings of QPSO are likely to be different. When solving engineering problems, the parameter setting of QPSO should be conservative to ensure that QPSO can converge as much as possible, instead of the fastest and best convergence [51].

Step 2. Calculate the weights and projection values by the PPM and QPSO.

The convergence curve of the PPM proposed in this paper obtained after program calculation is presented in Figure 2, from which it can be seen that QPSO converged between 100 and 200 generations. A detailed analysis of Figure 2 was carried out in section 5.

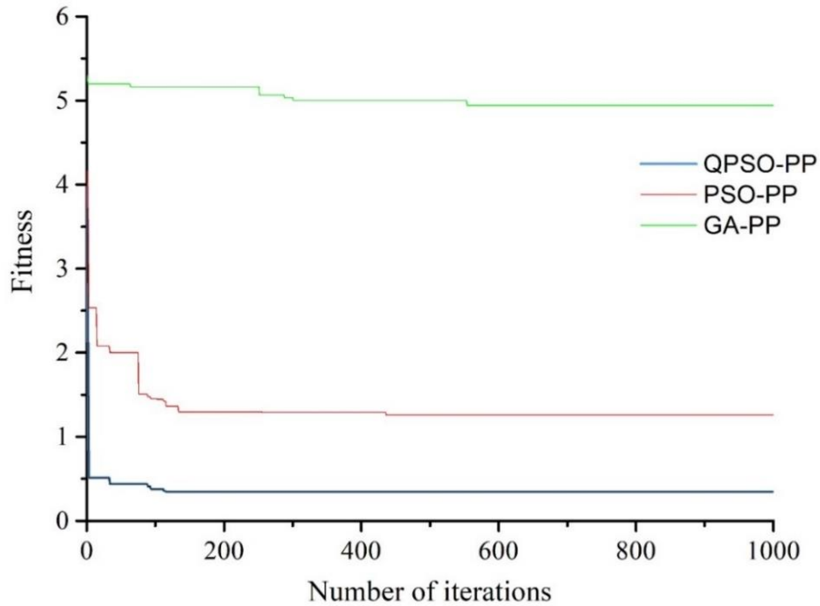

Figure 2. Convergence curves of QPSO-PP, PSO-PP, and GA-PP.

The fitness function of QPSO was tracked during each iteration, as showed in Table 5. Due to the length of the paper, we selectively listed some calculation results in combination with Figure 2. Before the 113th generation, the calculation errors of the fitness function were unacceptable, and a large number of calculation errors were larger than 0.00001. That is to say, before the 113th generation, the QPSO did not effectively find the optimal projection vector of PPM. In the 114 iterations, the calculation error of the fitness function was 0.000011218 > 0.0001, but the calculation error after 114 generations was less than 0.0001. After the 115th generation, the calculation errors of the fitness function were less than 0.00001. In other words, QPSO converged in the 115th generation. Combined with Figure 2, it can be considered that the objective function had been effectively optimized.

QPSO, a typical meta-heuristic algorithm, is a random algorithm. Because many operations are required in the optimization process, the calculation results may be unstable. Therefore, Step 1 and Step 2 were replicated ten times. In each calculation, the standard sample set $\mathbf{X_1}$ was randomly sampled again. The maximum and minimum standard deviations of the best projection value in the ten calculation results are presented in Table 6. In this case study, $n = 100$, and the maximum and minimum standard deviations of the best projection value were very small. When $n = 100$, the calculated results had good stability due to the sufficiently large amount of data. A detailed analysis of Table 6 was performed in the discussion in section 5.

Table 5. Precision level and calculation termination in the 1000th iteration.

Iteration (n)	Fitness (n-1)	Fitness (n)	Fitness (n) – Fitness (n−1)	Result
113	0.358670282	0.358670282	$0 < 0.00001$	Continue
114	0.166415693	0.166404475	$0.000011218 > 0.0001$	Continue
115	0.166404475	0.166404475	$0 < 0.0001$	Continue
1000	0.166404475	0.166404475	$0 < 0.0001$	Stop

Table 6. Stability analysis of the calculation results.

n	20	40	60	100	200
Maximum standard deviation	0.145853	0.0056	0.001116	0.000296352	0.000012839
Minimum standard deviation	0.005268	0.000351	0.00017	0.0000171668	0.00000038728

The optimum projection direction $\vec{\mathbf{a}}^* =$ (0.1513, 0.3317, 0.2161, 0.0954, 0.2086, 0.0990, 0.3817, 0.3305, 0.3661, 0.3489, 0.3915, 0.1817, 0.0173, 0.0300, 0.0400, 0.2419) was calculated by the program. The objective weight of each index was then obtained by squaring the numerical value of each element in the optimal projection vector.

Figure 3 presents the scatter diagram of the projection value set $\mathbf{Z_1}$ and corresponding recovery ability level set $\mathbf{Y_1}$ of 500 standard evaluation objects. In the figure, the abscissa is the best projection vector, and the ordinate is the restoring force level.

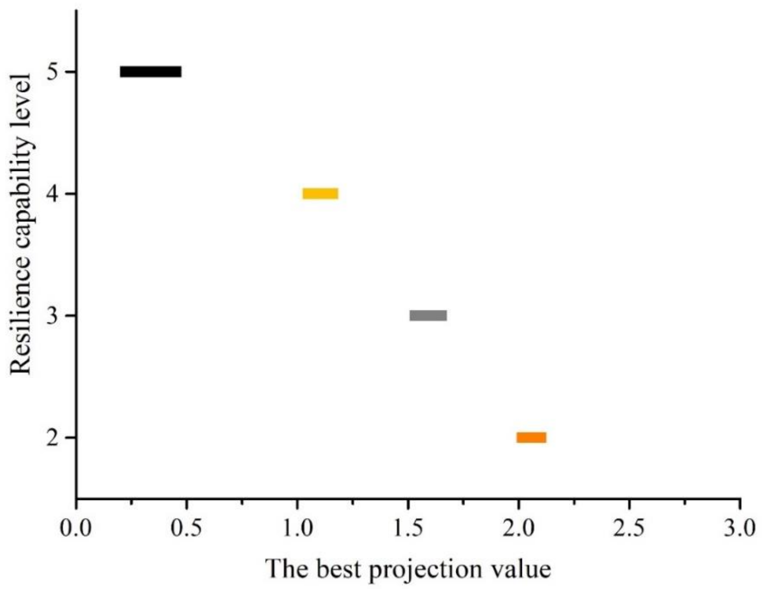

Figure 3. Scatter diagram of the projection values and resilience grades.

Step 3. Obtain the evaluation level by the interpolation algorithm.

Using the interpolation algorithm, the mathematical model is constructed as follows:

$$y = \begin{cases} 1 & z \geq 3.1737 \\ 1 + \dfrac{3.1737 - z}{3.1737 - 2.1015} & 2.1015 < z < 3.1737 \\ 2 & 2.0146 \leq z \leq 2.1015 \\ 2 + \dfrac{2.0146 - z}{2.0146 - 1.6526} & 1.6526 < z < 2.0146 \\ 3 & 1.5273 \leq z \leq 1.6526 \\ 3 + \dfrac{1.5273 - z}{1.5273 - 1.1610} & 1.1610 < z < 1.5273 \\ 4 & 1.0474 \leq z \leq 1.1610 \\ 4 + \dfrac{1.0474 - z}{1.0474 - 0.4595} & 0.4595 < z < 1.0474 \\ 5 & z \leq 0.4595 \end{cases} \tag{16}$$

By substituting the best projection values of the four station projects into Equation (16), their resilience levels could be calculated.

4.3. Analysis of calculation results

4.3.1. Analysis of weight calculation results

The objective weight of each index was obtained by squaring the numerical value of each element in the optimal projection vector λ^* calculated in section 4.2 [31]. The calculation results are reported in Table 7.

Table 7. Weight calculation results of secondary indicators.

Indicator	R11	R12	R13	R14	R15	R16	R21	R22
Weight	0.0229	0.1100	0.0467	0.0091	0.0435	0.0098	0.1457	0.1092
Ranking	11	5	8	13	9	12	2	6
Indicator	R23	R24	R25	R26	R31	R32	R33	R34
Weight	0.1340	0.1217	0.1533	0.0330	0.0003	0.0009	0.0016	0.0585
Ranking	3	4	1	10	16	15	14	7

R25 (Emergency plan of construction order) was found to have the largest weight, and has better interpretability. During the disaster recovery process in construction engineering, the emergency plan of construction order is the core of management, and all engineering and management measures for disaster recovery must be implemented in accordance with this recovery plan. R21 (Exercise frequency of the emergency plan) was found to have the second-largest weight. This is because the drilling of the emergency plan can reveal its shortcomings, can improve its rationality and feasibility of implementation, and is of great significance to improving the resilience of subway station projects to waterlogging disasters. Although the weight calculation results in this paper were obtained from the measured data of the construction site, they were well explained in combination with the practice of construction project management. This is the superiority of this research method compared with other objective weight calculation methods [52]. R23 (Relief supplies) ranked third in weight, which is easily understandable. Relief materials are the material basis for a subway station project to recover from a waterlogging disaster. R33 (Post-disaster technology update), R32 (Summary of post-disaster management), and R31 (Proportion of college students in project management personnel) were found to have the smallest weights.

The weights of the three primary indicators were obtained by summing the weights of the secondary indicators included in each primary indicator. The weights of R1 (Resistance), R2 (Recovery), and R3 (Adaptability) were respectively calculated to be 0.242, 0.6969, and 0.0613. This demonstrates that recovery is the most important indicator of the resilience of subway station projects to waterlogging disasters.

4.3.2. Analysis of resilience evaluation results

The best projection values of Lushan Avenue Station, Miaoeryan Station, Shenyang Road Station, and Tianfu CBD North Station were found to be 2.0353, 2.4691, 1.7135, and 1.5531, respectively. With the introduction of Eq (16), the values of the resilience of the four stations to rainstorm waterlogging disaster were calculated to be 2, 1.6571, 2.8318, and 3, respectively. Therefore, from greatest to least, the resilience ranking is Miaoeryan Station > Lushan Avenue Station > Shenyang Road Station > Tianfu CBD North Station. This ranking is consistent with the actual loss ranking of the four stations in the flood season of 2019, during which Shenyang Road Station and Tianfu CBD North Station suffered serious waterlogging disaster losses, and the construction period was delayed by about 45 days. In contrast, the waterlogging disaster loss of Lushan Avenue Station was small, and the construction period was delayed by about 15 days. Miaoeryan Station hardly suffered from any waterlogging disasters, and the construction period was not delayed. It should be pointed out that disaster losses in the engineering field are often determined by direct economic losses and casualties. The disaster recovery situation is expressed by the number of days of construction delay. The longer the construction delay, the more difficult it is for the project to overcome the disaster, and the lesser the resilience.

According to the division basis of the resilience grades presented in section 3.1.3, it is suggested that the management of rainstorm waterlogging disasters should be carried out at Miaoeryan Station and Lushan Avenue Station in accordance with the low-risk grade, whereas it should be carried out at Shenyang Road Station and Tianfu CBD North Station in accordance with the moderate-risk grade.

4.3.3. The calculation results of different optimization algorithms

The GA and classical PSO, which were two commonly used meta-heuristic algorithms as a benchmark comparison, were used to find the best projection vector of the PPM in the past research. In the GA, the number of individuals in the population was 50, the maximum genetic algebra was 1000, the binary digits were 20, and the generation gap was 0.9 [33]. In the PSO algorithm, the swarm size was 200, the personal learning coefficient and global learning coefficient were both 2, the inertia weights decreased linearly from 0.9 to 0.4, the minimum acceptance accuracy was 0.00001, and the maximum number of iterations was 1000 [34]. In addition to population size and convergence conditions, the key parameter required for QPSO is only the scaling coefficient, whereas the GA and PSO require more parameters. Compared with the GA and PSO, the QPSO has the advantage of fewer parameters.

In the analysis in section 4.2, it was not difficult to find that both the PSO and the GA had found the optimal solution. Bring the optimal solution found by the PSO or the GA into section 4.3.1 and section 4.3.2 for calculation. The calculation results are shown in Table 8.

Table 8. The values of the resilience obtained by different optimization algorithms.

Case	QPSO	PSO	GA
Lushan Avenue Station	2	2	2
Miaoeryan Station	1.6571	1.8931	1.9631
Shenyang Road Station	2.8318	2.7197	2.5678
Tianfu CBD North Station	3	3	3

It can be seen from Table 8 that the final calculation results of the three algorithms are almost the same. The restoration capacity of each station project was in the same order, but there was a certain difference in the restoration capacity grade value between the Miaoeryan Station and the Shenyang Road Station. Considering that many scholars [16,29] have prosperously used the PSO or the GA to optimize the PPM, the fact that the calculation results were basically the same could preliminarily prove the correctness of the calculation results in this paper.

The three algorithms, namely the GA, PSO, and QPSO, were compared in terms of the parameter setting, convergence speed, and the stability of calculation results. Due to the differences in parameter settings, it was impossible to compare the computing speeds of the three algorithms under the same parameters.

(1) *Parameter setting*. There are four parameters of the GA that needs to be set in advance. The population size was set to 100, the termination of the evolutionary algebra was set to 500, the crossover probability was set to 0.5, and the mutation probability was set to 0.001. Similarly, there are four parameters of the PSO that needs to be set in advance: the population size was set to 100, the acceleration coefficients C1 and C2 were set to 2, and the termination of the evolutionary algebra was set to 1000. However, only two parameters need to be set for QPSO, namely the population size and termination of evolutionary algebra. Therefore, as compared with the GA and PSO, fewer parameters need to be set for the QPSO.

(2) *Convergence speed*. It can be observed in Figure 2 that the QPSO found the best projection vector between 100 and 200 generations, whereas the classical PSO found the best projection vector between 200 and 300 generations. The convergence speed of the GA was the slowest, and it took about 500-600 generations to find the best projection vector. By tracking the calculation processes of the PSO and GA, it was found that the PSO converged after 256 generations and the GA converged after 556 generations. In this case study, the QPSO exhibited a faster convergence speed, which is in agreement with the analysis results in previous research [23,24,32–34]. This further illustrates the superiority of the QPSO, and proves the rationality of the research results in this paper to a certain extent.

(3) *Stability of calculation results*. Although the QPSO, the PSO, and the GA had found the optimal solution, the stability of the calculated results might be different. The 5-fold cross-validation [53] and the analysis of variance (ANOVA) [54,55] are commonly used detection methods. In this paper, variance analysis is selected according to the characteristics of data. In this paper, the QPSO, the PSO, and the GA were used to analyze cases 200 times. The standard deviations of 200 calculation results

of the three optimization algorithms are shown in Table 9.

Table 9. Standard deviation of calculation results of three optimization algorithms.

Case	QPSO	PSO	GA
Lushan Avenue Station	0.000155318	0.0012241	0.03189
Miaoeryan Station	0.000139837	0.002564	0.031891
Shenyang Road Station	0.000168777	0.0051055	0.03076
Tianfu CBD North Station	0.000126528	0.0102063	0.025302

In the Table 9, the standard deviation of the calculation results of QPSO is obviously smaller than that of PSO or GA, which also proves that the stability of QPSO is better than that of PSO and GA. Taking the calculation results of Miaoeryan Station as an example, the GA incorrectly calculated the station's resilience level as 2 for 7 times in 200 calculations, PSO algorithm for 3 times, and QPSO algorithm for none. The fundamental reason for this was that particles were able to appear at any position in the solution space in QPSO algorithm, which effectively avoided the problem of finding the local optimal solution [23,24].

5. Discussions

In this work, the PPM improved by QPSO was developed to evaluate the resilience of subway station projects to rainstorm waterlogging disasters. However, the following limitations existed. (1) The influences of different index systems on the resilience evaluation results are not discussed. (2) The temporal and spatial evolution characteristics of the waterlogging disaster recovery ability of subway station projects are not deeply analyzed or revealed. (3) The covariance matrix adaptation evolutionary strategies (CMA-ES) [56], the coyote optimization algorithm (COA) [57], and other state-of-art approaches are suggested to solve the optimization problem of PPM.

5.1. Comparative analysis of different evaluation methods

At present, fuzzy comprehensive evaluation method and AHP method are commonly used to evaluate the resilience of waterlogging disasters in subway station projects [13,14]. The basic idea of these studies is to use the AHP method to calculate the weights, and then use fuzzy comprehensive evaluation method to calculate the resilience grade. This section analyzed and compared the calculation results of these traditional methods with the model proposed in this paper, in order to highlight the progressiveness of the model proposed in this paper.

The theory and the calculation process of AHP could refer to the relevant research results [13,14], so we would not repeat them here. In this paper, 20 experts in the Section 4 were selected and divided into 4 groups. The calculation results of weights calculated by the AHP method are shown in Table 10.

It could be clearly seen from Table 10 that the index weights calculated by four groups of experts were obviously different. This difference was determined by the subjectivity of the AHP method. Due to the large number of indicators, it took many expert questionnaires to pass the consistency test when using the AHP method to calculate the weight of each indicator. In this paper, the PPM was used to calculate the optimal projection vector to obtain the weights, which was an objective calculation method based on the data-driven. The PPM determined the index weight according to the quantitative and qualitative data actually obtained from the construction site, instead of the subjective judgment on the importance of the index.

The theory and the calculation process of fuzzy comprehensive evaluation could refer to previous research results [13]. The key work of fuzzy comprehensive evaluation method was to beforehand determine the membership function according to the experience and judgment of experts before evaluation. Obviously, this method of presetting membership functions was greatly influenced by subjective factors of experts, and the calculation results of different membership functions might be different. In this paper, 20 experts in the section 4 were selected and divided into four groups. Four groups of experts set different membership functions [13], and the calculation results are shown in Table 11.

Table 10. Weight calculation results of the AHP method.

Indicators	First group		Second group		Third group		Fourth group	
	Weight	Ranking	Weight	Ranking	Weight	Ranking	Weight	Ranking
R11	0.0458	12	0.0291	11	0.0681	7	0.0145	14
R12	0.0147	16	0.0096	16	0.0743	4	0.0087	16
R13	0.0527	8	0.0781	5	0.0155	15	0.0221	9
R14	0.0275	13	0.0545	7	0.0591	9	0.0156	12
R15	0.0556	6	0.0452	9	0.0486	11	0.0174	10
R16	0.0556	5	0.0559	6	0.1759	1	0.0147	13
R21	0.1133	2	0.0332	10	0.0735	6	0.0928	4
R22	0.0208	15	0.0277	13	0.0218	13	0.0239	8
R23	0.0647	4	0.0261	14	0.0487	10	0.0345	6
R24	0.0540	7	0.0278	12	0.0998	3	0.0166	11
R24	0.0510	10	0.0498	8	0.0374	12	0.0091	15
R26	0.0523	9	0.0181	15	0.0622	8	0.0442	5
R31	0.1068	3	0.1059	2	0.0218	14	0.3124	1
R32	0.0239	14	0.1059	3	0.0128	16	0.2308	2
R33	0.0477	11	0.2335	1	0.0742	5	0.1075	3
R34	0.2136	1	0.1059	4	0.1063	2	0.0343	7

Table 11. Results of resilience level by the fuzzy comprehensive evaluation.

Case	First group	Second group	Third group	Fourth group
Lushan Avenue Station	2	2	2	2
Miaoeryan Station	1	2	1	1
Shenyang Road Station	3	2	2	3
Tianfu CBD North Station	3	3	3	3

The membership functions set by the four groups of experts were different, so the calculation results were obviously different in the Table 11. Experts in the first group, the third group, and the fourth group thought that the restoration ability of Miaoeryan Station was 1, while experts in the second group thought that the restoration ability of Miaoeryan Station was 2. In addition, the fuzzy comprehensive evaluation was not able to make full use of a large number of measured data. However, the new model in this paper could directly use a large number of measured data, and adopt the method of data-driven rather than subjective judgment of experts.

In addition, compared with the calculation results of the model proposed in this paper, it was considered that the resolution of the calculation results by the AHP and the fuzzy comprehensive evaluation was poor. According to the calculation results of the first group of experts, the recoverability levels of Shenyang Road Station and Tianfu CBD North Station were 3, and the calculation results of the second group of experts showed that the recoverability levels of Lushan Avenue Station, Miaoeryan Station, and Shenyang Road Station were 2. This was due to the fine mathematical model constructed by interpolation algorithm in this paper.

5.2. *The influence of the number of indicators on the calculation results*

In the researches of disaster risk or resilience evaluation, the selection of indicators has a significant impact on the calculation results. According to the definition of subway waterlogging disaster resilience in the introduction and the typical subway waterlogging disasters, the index system in Table 1 was constructed. This index system included 3 primary indicators and 16 secondary indicators. If different typical projects were selected for analysis, the index system of resilience would be different. It is worth mentioning that there is almost no research on the resilience of subway to resist floods or disasters. In the case analysis of this paper, this index system had achieved good research results. Therefore, this section would not study the influence of adding secondary indicators on the calculation results. This section mainly discussed the influence of deleting secondary indicators on calculation results, in order to find the smallest indicator set.

The evaluation results after deleting any secondary index were calculated in detail. For reasons of space, only some calculation results are listed in Table 12. The calculation results showed that deleting a secondary index would hardly change the calculation results, the restoration ability grades, and restoration ability rankings of four typical station projects. However, when the index R25 or R21 was deleted, the change of calculation result was the biggest. This was consistent with the weight calculation results in section 4.3.1. R25 and R21 were the two indexes with the greatest weights, and should also have the greatest influence on the calculation results [58].

This paper also calculated the evaluation results after arbitrarily deleting two indicators, as shown in Table 12. The calculation results showed that deleting two secondary indexes might cause changes in the calculation results. Among them, the indexes R21 and R25 were deleted, and the indexes R21 and R23 were deleted. In these two cases, the calculation results would change and the resolution of which calculation results would decrease. It could be preliminarily considered that the reduction of input indexes led to the reduction of the computational resolution of the model. This was also consistent with the weight calculation results in section 4.3.1. R21, R23 and R25 were the three secondary indexes with the greatest weights, which should also have the greatest influence on the calculation results [58]. Therefore, on the basis of the index system in section 3.1, deleting one index would not change the calculation result, while deleting two indexes might change the calculation result. However, this conclusion needed more case studies to support it.

Because the author's research time and materials were limited, this paper did not make further analysis on the number of indicators. However, with the continuous enrichment of related research results, a unified and applicable evaluation index of subway flood disaster resilience would be formed.

Table 12. Calculation results after deleting some secondary indicators.

Case name	Lushan Avenue Station	Miaoeryan Station	Shenyang Road Station	Tianfu CBD North Station
Deleting R21	2	1.7637	2.5610	3
Deleting R25	2	1.7562	2.7536	3
Deleting R21 and R25	2	2	3	3
Deleting R21 and R23	2	2	3	3

5.3. *Influences of different random sampling numbers on the calculation results*

A data-mining method was proposed in this work, and the data characteristics had a great influence on the calculation results. In section 3.2.3, *N* standard samples were generated in each grade interval by random sampling. By choosing a different value of *n*, different standard sample sets can be obtained. In the case study analysis, $n = 100$ was easily set. In fact, while many similar research works [6,42] directly provided the value of *n* when using the interpolation algorithm, they did not analyze the influences of different values of n on the calculation results. Therefore, four cases of $n = 20, 40, 60, 200$ were calculated, and the influences of the different values of n on the calculation results were investigated.

After calculation in the four cases of $n = 20, 40, 60, 200$, the characteristics of the $\mathbf{Z_1}$ and $\mathbf{Y_1}$ scatter plots were found to be similar to those of $n = 100$, and they were all descending line segments. The mathematical models constructed under the three conditions of $n = 20, 40, 60$ were quite different from those constructed under the condition of $n = 100$.

When $n = 20$, the mathematical model is as follows:

$$y = \begin{cases} 1 & z \geq 2.9250 \\ 1 + \dfrac{2.9250 - z}{2.9250 - 2.2829} & 2.2829 < z < 2.9250 \\ 2 & 2.1355 \leq z \leq 2.2829 \\ 2 + \dfrac{2.1355 - z}{2.1355 - 1.8043} & 1.8043 < z < 2.1355 \\ 3 & 1.6476 \leq z \leq 1.8043 \\ 3 + \dfrac{1.6476 - z}{1.6476 - 1.2562} & 1.2562 < z < 1.6476 \\ 4 & 1.1172 \leq z \leq 1.2562 \\ 4 + \dfrac{1.1172 - z}{1.1172 - 0.6923} & 0.6923 < z < 1.1172 \\ 5 & z \leq 0.6923 \end{cases} \tag{17}$$

The best projection values of Lushan Avenue Station, Miaoeryan Station, Shenyang Road Station, and Tianfu CBD North Station were found to be 2.1709, 2.6830, 1.6574, and 1.7698, respectively. With the introduction of Eq (17), the values of the resilience of the four stations to rainstorm waterlogging disasters were calculated as 2, 1.3769, 3, and 3 respectively. Therefore, the resilience ranking is Miaoeryan Station > Lushan Avenue Station > Shenyang Road Station = Tianfu CBD North Station. However, according to the order of the best projection values, Shenyang Road Station > Tianfu CBD North Station. The calculation results when *n* = 20 are consistent with the actual loss ranking of the four stations in the flood season of 2019. However, as compared with the model when *n* = 100, this mathematical model has poor resolution.

According to the results in Table 6, when $n = 20$, the maximum standard deviation of ten calculation results was 0.145853, and the minimum standard deviation was 0.005268. In other words, when $n = 20$, the calculation result of the optimal projection value is very unstable [59].

When $n = 40$, the mathematical model is as follows:

$$y = \begin{cases} 1 & z \geq 2.9064 \\ 1 + \dfrac{2.9064 - z}{2.9064 - 2.2225} & 2.2225 < z < 2.9064 \\ 2 & 2.0307 \leq z \leq 2.2225 \\ 2 + \dfrac{2.0307 - z}{2.0307 - 1.7415} & 1.7415 < z < 2.0307 \\ 3 & 1.5404 \leq z \leq 1.7415 \\ 3 + \dfrac{1.5404 - z}{1.5404 - 1.2299} & 1.2299 < z < 1.5404 \\ 4 & 1.0709 \leq z \leq 1.2299 \\ 4 + \dfrac{1.0709 - z}{1.0709 - 0.6071} & 0.6071 < z < 1.0709 \\ 5 & z \leq 0.6071 \end{cases} \tag{18}$$

The best projection values of Lushan Avenue Station, Miaoeryan Station, Shenyang Road Station, and Tianfu CBD North Station were found to be 2.0913, 2.7065, 1.9700, and 1.6921, respectively. With the introduction of Eq (18), the values of the resilience of the four stations to rainstorm waterlogging disasters were calculated as 2, 1.2923, 2.2099, and 3, respectively. Therefore, the resilience ranking is Miaoeryan Station > Lushan Avenue Station > Shenyang Road Station > Tianfu CBD North Station. The calculation results when $n = 40$ are consistent with the actual loss ranking of the four stations in the flood season of 2019. According to the results in Table 6, when $n = 40$, the maximum standard deviation of ten calculation results was 0.0056, and the minimum standard deviation was 0.000351. Although the standard deviation was smaller when $n = 40$ than when $n = 20$, the calculated results were always unstable.

When $n = 60$, the mathematical model is as follows:

$$y = \begin{cases} 1 & z \geq 2.9706 \\ 1 + \dfrac{2.9706 - z}{2.9706 - 2.2695} & 2.2695 < z < 2.9706 \\ 2 & 2.042 \leq z \leq 2.2695 \\ 2 + \dfrac{2.042 - z}{2.042 - 1.7515} & 1.7515 < z < 2.042 \\ 3 & 1.5725 \leq z \leq 1.7515 \\ 3 + \dfrac{1.5725 - z}{1.5725 - 1.2689} & 1.2689 < z < 1.5725 \\ 4 & 1.1032 \leq z \leq 1.2689 \\ 4 + \dfrac{1.1032 - z}{1.1032 - 0.6366} & 0.6366 < z < 1.1032 \\ 5 & z \leq 0.6366 \end{cases} \tag{19}$$

The best projection values of Lushan Avenue Station, Miaoeryan Station, Shenyang Road Station, and Tianfu CBD North Station were found to be 2.1136, 2.8378, 1.9482, and 1.7253, respectively.

With the introduction of Eq (19), the values of the resilience of the four stations to rainstorm waterlogging disasters were calculated as 2, 1.1895, 2.3238, and 3, respectively. Therefore, the resilience ranking is Miaoeryan Station > Lushan Avenue Station > Shenyang Road Station > Tianfu CBD North Station. The calculation results when $n = 60$ are consistent with the actual loss ranking of the four stations in the flood season of 2019. According to the results in Table 6, when $n = 60$, the maximum standard deviation of ten calculation results was 0.001116, and the minimum standard deviation was 0.00017. It can therefore be considered that the calculation results were stable when $n = 60$.

When $n = 200$, the mathematical model was almost identical to that when $n = 100$. Additionally, the maximum standard deviation was 0.000012839 and the minimum standard deviation was 0.0000038729, which are much smaller than those when $n = 100$. However, when $n = 200$, the data dimension is too high and the calculation time is very long. Thus, $n = 100$ is reasonable.

By comprehensively comparing the preceding analysis results, it is evident that different random sampling numbers will lead to different mathematical models for resilience evaluation, which may have a certain influence on the evaluation results. However, regarding the present case study, high accuracy and stability can be achieved when $n = 100$.

6. Conclusions

Considering the weaknesses of disaster management evaluation methods and the lack of research on the resilience of subway station projects to rainstorm waterlogging disasters, an evaluation PPM was constructed based on QPSO. Sixteen secondary indexes that affected the ability of subway station projects to recover from waterlogging disasters were identified from defense, recovery, and adaptability. The assessment standard of 16 secondary indexes was provided in combination with the Chengdu Metro Line 11 project. The QPSO, PPM, and interpolation algorithm were used to construct an evaluation model of the ability of subway station projects to recover from waterlogging disasters. In this model, the PPM was utilized to effectively deal with the high-dimensional data, and QPSO was used to solve the best projection vector of the PPM, which effectively solved the shortcoming of the traditional PSO easily falling into the local extremum due to its limited search space. In addition, a case study analysis of four typical station projects of Chengdu Metro Line 11 was conducted, and it was found that the key influencing factors of the ability of subway station projects to recover from rainstorm waterlogging disasters are the emergency plan of construction order, the exercise frequency of the emergency plan, and the relief supplies. Moreover, recovery was considered to be the most important indicator. The values of the resilience of Lushan Avenue Station, Miaoeryan Station, Shenyang Road Station, and Tianfu CBD North Station to rainstorm waterlogging disasters were found to be 2, 1.6571, 2.8318, and 3, respectively. The resilience ranking of the four stations was consistent with their waterlogging loss ranking in the flood season of 2019, which proved the reliability and effectiveness of the proposed model. In addition, two classical meta-heuristic algorithms, PSO and GA, were also used to solve the optimal projection vector of PPM, and the calculation results demonstrated that QPSO had the advantages of fewer parameter settings and a fast convergence speed, which also proved the superiority of the proposed model.

However, the following limitations existed. The influences of different index systems on the resilience evaluation results are not discussed. The temporal and spatial evolution characteristics of the waterlogging disaster recovery ability of subway station projects are not deeply analyzed or revealed. The in-depth analysis and revelation of the temporal and spatial evolution characteristics of the ability of subway station projects to recover from waterlogging disasters, are worthy of future research. The PPM could reduce the complexity of data and ensure the accuracy and robustness of data processing. How to construct projection objective function by using sample aggregation degree and inter-class dispersion degree is the key to correct use of PPM. Moreover, solving the projection objective function is a typical complex nonlinear optimization problem. There will be more meta-heuristic algorithms used to solve the objective function in future research.

Acknowledgments

This paper is supported by the Science and Technology Project of Wuhan Urban and Rural Construction Bureau, China (201943).

Conflict of interest

The authors declare there is no conflict of interest.

References

1. T. Lin, X. F. Liu, J. C. Song, G. Q. Zhang, Y. Q. Jia, Z. Z. Tu, et al., Urban waterlogging risk assessment based on internet open data: A case study in China, *Habitat Int.*, **71** (2018), 88–96.
2. H. Y. Yu, C. Liang, P. Li, K. J. Niu, F. X. Du, J. H. Shao, et al., Evaluation of Waterlogging Risk in an Urban Subway Station, *Adv. Civ. Eng.*, **2019** (2019), 1–12.
3. Z. E. Yin, J. Yin, S. Y. Xu, J. H. Wen, Community-based scenario modelling and disaster risk assessment of urban rainstorm waterlogging, *J. Geogr. Sci.*, **21** (2011), 274–284.
4. S. L. Cutter, K. D. Ash, C. T. Emrich, Urban–Rural Differences in Disaster Resilience, *Ann. Am. Assoc. Geogr.*, **106** (2016), 1236–1252.
5. W. L. Lai, H. R. Wang, C. Wang, J. Zhang, Y. Zhao, Waterlogging risk assessment based on self-organizing map (SOM) artificial neural networks: a case study of an urban storm in Beijing, *J Mt. Sci.*, **14** (2017), 898–905.
6. H. Wu, J. W. Wang, Assessment of Waterlogging Risk in the Deep Foundation Pit Projects Based on Projection Pursuit Model, *Adv. Civ. Eng.*, **2020** (2020).
7. B. L. Turner, R. E. Kasperson, P. A. Matson, J. J. McCarthy, R. W. Corell, L. Christensen, et al., A framework for vulnerability analysis in sustainability science, *Proc. Natl. Acad. Sci. U. S. A.*, **100** (2003), 8074–8079.
8. S.Hunt, M. Eburn, How Can Business Share Responsibility for Disaster Resilience, *Aust. J. Public Adm.*, **77** (2018), 482–491.
9. W. N. Adger, T. P. Hughes, C. Folke C, S. R. Carpenter, J. Rockstrom, Social-Ecological Resilience to Coastal Disasters, *Science*, **309** (2005), 1036–1039.
10. A. Bozza, D. Asprone, F. Fabbrocino F, Urban Resilience: A Civil Engineering Perspective, *Sustainability*, **9** (2017), 103.
11. R. Leichenko, Climate change and urban resilience, *Curr. Opin. Environ. Sustain.*, **3** (2011), 164–168.

12. S. Qasim, M. Qasim, R. P. Shrestha, A. N. Khan, K. Tune, M. Ashraf, Community resilience to flood hazards in Khyber Pukhthunkhwa province of Pakistan, *Int. J. Disaster Risk Reduct.*, **18** (2016), 100–106.
13. Y. M. Liu, C. Lu, X. M. Yang, Z. H. Wang, B. Liu, Fine-Scale Coastal Storm Surge Disaster Vulnerability and Risk Assessment Model: A Case Study of Laizhou Bay, China, *Remote Sens.*, **12** (2020), 1301.
14. G. F. Li, X. Y. Xiang, Y. Y. Tong, H. M. Wang, Impact assessment of urbanization on flood risk in the Yangtze River Delta, *Stoch. Environ. Res. Risk Assess.*, **27** (2013), 1683–1693.
15. S. Ayesha, M. K. Hanif, R. Talib, Overview and comparative study of dimensionality reduction techniques for high dimensional data, *Inf. Fusion,* **59** (2020), 44–58.
16. G. Z. Zhi, Z. L. Liao, W. C. Tian, J. Wu, Urban flood risk assessment and analysis with a 3D visualization method coupling the PP-PSO algorithm and building data, *J. Environ. Manage.*, **268** (2020), 110521.
17. N. Suwal, X. F. Huang, A. Kuriqi, Y. Q. Chen, K. P. Pandey, K. P. Bhattarai, Optimisation of cascade reservoir operation considering environmental flows for different environmental management classes, *Renew. Energy*, **158** (2020), 453–464.
18. A. Berro, S. L. Marie-Sainte, A. Ruiz-Gazen, Genetic algorithms and particle swarm optimization for exploratory projection pursuit, *Ann. Math. Artif. Intell.*, **60** (2010), 153–178.
19. H. Yoshida, K. Kawata, Y. Fukuyama, S. Takayama, Y. Nakanishi, A particle swarm optimization for reactive power and voltage control considering voltage security assessment, *IEEE Trans. Power Syst.*, **15** (2000), 1232–1239.
20. S. Chalermchaiarbha, W. Ongsakul, Elitist Multi-objective Particle Swarm Optimization with Fuzzy Multi-attribute Decision Making for Power Dispatch, *Electr. Power Compon. Syst.*, **40** (2012), 1562–1585.
21. W. Elloumi, N. Baklouti, A. Abraham, A. M. Alimi, The multi-objective hybridization of particle swarm optimization and fuzzy ant colony optimization, *J. Intell. Fuzzy Syst.*, **27** (2014), 515–525.
22. J. Sun, B. Feng, W. Xu, *Particle swarm optimization with particles having quantum behavior*, 2004 Congress on Evolutionary Computation, 2004. Available from: https://ieeexplore.ieee.org/document/1330875.
23. K. Meng, H. G. Wang, Z. Y. Dong, K. P. Wong, Quantum-Inspired Particle Swarm Optimization for Valve-Point Economic Load Dispatch, *IEEE Trans. Power Syst.*, **25** (2010), 215–222.
24. Q. Q. Zhang, S. F. Liu, D. Q. Gong, H. K. Zhang, Q. Tu, An Improved Multi-Objective Quantum-Behaved Particle Swarm Optimization for Railway Freight Transportation Routing Design, *IEEE Access.*, **7** (2019), 157353–157362.
25. J. J. Zeng, G. R. Huang, Set pair analysis for karst waterlogging risk assessment based on AHP and entropy weight, *Hydrol. Res.*, **49** (2018), 1143–1155.
26. A. Y. Lo, B. X. Xu, B. F. Chan, R. X. Su, Household economic resilience to catastrophic rainstorms and flooding in a Chinese megacity, *Geogr. Res.*, **54** (2016), 406–419.
27. H. M. Lyu, Y. S. Xu, W. C. Cheng, A. Arulrajah, Flooding Hazards across Southern China and Prospective Sustainability Measures, *Sustainability*, **10** (2018), 1682.
28. P. Cui, D. Z. Li, Measuring the Disaster Resilience of an Urban Community Using ANP-FCE Method from the Perspective of Capitals, *Soc. Sci. Q.*, **100** (2019), 2059–2077.

29. S. J. Wang, X. L. Zhang, Z. F. Yang, J. Ding, Z. Y. Shen, Projection pursuit cluster model based on genetic algorithm and its application in Karstic water pollution evaluation, *Int. J. Environ. Pollut.*, **28** (2006), 253–260.
30. J. W. Gong, C. M. Jiang, X. J. Tang, Z. G. Zheng, L. X. Yang, Optimization of mixture proportions in ternary low-heat Portland cement-based cementitious systems with mortar blends based on projection pursuit regression, *Constr. Build. Mater.*, **238** (2020), 117666.
31. Z. G. Lan, M. Huang, Safety assessment for seawall based on constrained maximum entropy projection pursuit model. *Nat. Hazards*, **91** (2018), 1165–1178.
32. D. Yumin, Z. Li, Quantum Behaved Particle Swarm Optimization Algorithm Based on Artificial Fish Swarm, *Math. Probl. Eng.*, **2014** (2014), 592682.
33. W. Fang, J. Sun, Y. R. Ding, X. J. Wu, W. B. Xu, A Review of Quantum-behaved Particle Swarm Optimization, *IETE Tech. Rev.*, **27** (2010), 336–348.
34. Y. G. Fu, M. Y. Ding, C. P. Zhou, Phase Angle-Encoded and Quantum-Behaved Particle Swarm Optimization Applied to Three-Dimensional Route Planning for UAV, *IEEE Trans. Syst. Man Cybern. Part A Syst. Hum.*, **42** (2012), 511–526.
35. K. Yang, W. M. Feng, G. Liu, J. F. Zhao, P. Y. Su, Quantum-behaved particle swarm optimization for far-distance rapid cooperative rendezvous between two spacecraft, *Adv. Space Res.*, **62** (2018), 2998–3011.
36. H. Talbi, A. Draa, A new real-coded quantum-inspired evolutionary algorithm for continuous optimization, *Appl. Soft. Comput.*, **61** (2017), 765–791.
37. H. Khodadadi, S. Vatankhah, T. Sadeghi, Indexes of caring for elderly in earthquakes according to the Iranian experience: a qualitative study, *Dis. Med. Public Health Prep.*, **12** (2018), 493–501.
38. M. S. Chang, Y. L. Tseng, J. W. Chen, A scenario planning approach for the flood emergency logistics preparation problem under uncertainty, *Transp. Res. Part E Logist. Transp. Rev.*, **43** (2007), 737–754.
39. W. Yi, L. Ozdamar, A dynamic logistics coordination model for evacuation and support in disaster response activities, *Eur. J. Oper. Res.*, **179** (2007), 1177–1193.
40. D. Liu, J. P. Feng, H. Li, Q. Fu, M. Li, M. A. Faiz, et al., Spatiotemporal variation analysis of regional flood disaster resilience capability using an improved projection pursuit model based on the wind-driven optimization algorithm, *J. Clean Prod.*, **241** (2019), 118406.
41. S. F. Ardabili, B. Najafi, S. Shamshirband, B. M. Bidgoli, R. C. Deo, K. W. Chau, Computational intelligence approach for modeling hydrogen production: a review, *Eng. Appl. Comp. Fluid Mech.*, **12** (2018), 438–458.
42. R. Taormina, K. W. Chau, ANN-based interval forecasting of streamflow discharges using the LUBE method and MOFIPS, *Eng. Appl. Artif. Intell.*, **45** (2015), 429–440.
43. J. Sun, X. J. Wu, V. Palade, W. Fang, C. H. Lai, W. B. Xu, Convergence analysis and improvements of quantum-behaved particle swarm optimization, *Inf. Sci.*, **192** (2012), 81–103.
44. M. S. Alajmi, A. M. Almeshal, Prediction and Optimization of Surface Roughness in a Turning Process Using the ANFIS-QPSO Method, *Materials*, **13** (2020), 2986.
45. G. G. Wang, A. H. Gandomi, A. H. Alavi, S. Deb, A hybrid method based on krill herd and quantum-behaved particle swarm optimization, *Neural Comput. Appl.*, **27** (2016), 989–1006.
46. X. H. Yang, Z. F. Yang, Z. Y. Shen, et al, Interpolation model for flood disaster assessment based on projection pursuit, *Disaster Sci.*, **04** (2004), 3–8.

47. C. L. Wu, K. W. Chau, Prediction of rainfall time series using modular soft computing methods, *Eng. Appl. Artif. Intell.*, **26** (2013), 997–1007.
48. V. R. Renjith, G. Madhu, V. L. J. Nayagam, A. B. Bhasi, Two-dimensional fuzzy fault tree analysis for chlorine release from a chlor-alkali industry using expert elicitation, *J. Hazard. Mater.*, **183** (2010), 103–110.
49. M. H. P. Passos, H. A. Silva, A. C. R. Pitangui, V. M. A. Oliveira, A. S. Lima, R. C. Araujo, Reliability and validity of the Brazilian version of the Pittsburgh Sleep Quality Index in adolescents, *J. Pediatr.*, **93** (2017), 200–206.
50. C. T. Cheng, W. J. Niu, Z. K. Feng, J. J. Shen, K. W. Chau, Daily reservoir runoff forecasting method using artificial neural network based on quantum-behaved particle swarm optimization, *Water*, **7** (2015), 4232–4246.
51. J. Derrac, S. Garcia, S. Hui, P. N. Suganthan, F. Herrera, Analyzing convergence performance of evolutionary algorithms: A statistical approach, *Inf. Sci.*, **289** (2014), 41–58.
52. B. Ji, Y. Ye, Y. Xiao, A combination weighting algorithm using relative entropy for document clustering, *Int. J. Pattern Recognit. Artif. Intell.*, **28** (2014), 1453002.
53. A. Banan, A. Nasiri, A. Taheri-Garavand, Deep learning-based appearance features extraction for automated carp species identification, *Aquac. Eng.*, **89** (2020), 102053.
54. A. Czarn, C. MacNish, K. Vijayan, B. Turlach, R. Gupta, Statistical exploratory analysis of genetic algorithms, *IEEE Trans. Evol. Comput.*, **8** (2004), 405–421.
55. J. Carrasco, S. Garcia, M. M. Rueda, S. Das, F. Herrera, Recent trends in the use of statistical tests for comparing swarm and evolutionary computing algorithms: Practical guidelines and a critical review, *Swarm Evol. Comput.*, **54** (2020), 10066.
56. C. Igel, N. Hansen, S. Roth, Covariance matrix adaptation for multi-objective optimization, *Evol. Comput.*, **15** (2007), 1–28.
57. V. J, Chin, Z. Salam, Coyote optimization algorithm for the parameter extraction of photovoltaic cells, *Sol. Energy*, **194** (2019), 656–670.
58. M. Wang, N. C. Chang, J. B. Liu et al., A multi-index comprehensive evolution method of state estimation, *Auto Elec. Power Syst.*, **39** (2015), 94–98.
59. B. A. Hassan and T. A. Rashid, Datasets on statistical analysis and performance evaluation of backtracking search optimisation algorithm compared with its counterpart algorithms, *Data Brief*, **28** (2020), 105046.